JOURNAL OF VIROLOGY, Feb. 2000, p. 1393–1406 Vol. 74, No. 3
0022-538X/00/$04.00+0

Retargeting of Coronavirus by Substitution of the Spike Glycoprotein Ectodomain: Crossing the Host Cell Species Barrier

LILI KUO,[1] GERT-JAN GODEKE,[2] MARTIN J. B. RAAMSMAN,[2] PAUL S. MASTERS,[1]* AND PETER J. M. ROTTIER[2]

David Axelrod Institute, Wadsworth Center for Laboratories and Research, New York State Department of Health, Albany, New York 12201,[1] and Institute of Virology, Department of Infectious Diseases and Immunology, Faculty of Veterinary Medicine, and Institute of Biomembranes, Utrecht University, 3584 CL Utrecht, The Netherlands[2]

Received 8 July 1999/Accepted 25 October 1999

Coronaviruses generally have a narrow host range, infecting one or just a few species. Using targeted RNA recombination, we constructed a mutant of the coronavirus mouse hepatitis virus (MHV) in which the ectodomain of the spike glycoprotein (S) was replaced with the highly divergent ectodomain of the S protein of feline infectious peritonitis virus. The resulting chimeric virus, designated fMHV, acquired the ability to infect feline cells and simultaneously lost the ability to infect murine cells in tissue culture. This reciprocal switch of species specificity strongly supports the notion that coronavirus host cell range is determined primarily at the level of interactions between the S protein and the virus receptor. The isolation of fMHV allowed the localization of the region responsible for S protein incorporation into virions to the carboxy-terminal 64 of the 1,324 residues of this protein. This establishes a basis for further definition of elements involved in virion assembly. In addition, fMHV is potentially the ideal recipient virus for carrying out reverse genetics of MHV by targeted RNA recombination, since it presents the possibility of selecting recombinants, no matter how defective, that have regained the ability to replicate in murine cells.

The family *Coronaviridae* contains the causative agents of a number of significant respiratory and enteric diseases affecting humans, other mammals, and birds (55). One of the hallmarks of this family is that most of its members exhibit a very strong degree of host species specificity, the molecular basis of which is thought to reside in the particularity of the interactions of individual viruses with their corresponding host cell receptors.

Coronaviruses have positive-stranded RNA genomes, on the order of 30 kb in length, that are packaged by a nucleocapsid protein (N) into helical ribonucleoprotein structures (31). The nucleocapsid is incorporated into viral particles by budding through the membrane of the intermediate compartment between the endoplasmic reticulum and the Golgi complex (26, 57). Subsequent to budding, it may acquire a spherical, possibly icosahedral superstructure (43, 44). The virion envelope surrounding the nucleocapsid contains a minimal set of three structural proteins: the membrane glycoprotein (M), the small envelope protein (E), and the spike glycoprotein (S). In some coronaviruses, other proteins may also be present; these include a hemagglutinin-esterase (HE) (34, 54) and the product of the internal open reading frame of the N gene (I protein) (12, 53), neither of which is essential for virus infectivity.

M is the most abundant of the virion structural proteins. It spans the membrane bilayer three times, having a short amino-terminal domain on the exterior of the virus and a large carboxy terminus, containing more than half the mass of the molecule, in the virion interior (48). By contrast, E is a minor structural protein, in both size and stoichiometry, and was only relatively recently identified as a constituent of viral particles (17, 33, 62). The most prominent virion protein, S, makes a single pass through the membrane envelope, with almost the entire molecule forming an amino-terminal ectodomain. Multimers of S make up the large peplomers, characteristic of coronaviruses, that recognize cellular receptors and mediate fusion to host cells.

Although the details of the coronavirus assembly process are not yet understood, major progress in elucidating the molecular interactions that determine the formation and composition of the virion envelope has been made in the past few years. Much of this has been driven by the demonstration that in the absence of viral infection, coexpression of the M, E, and S proteins results in the assembly of coronavirus-like particles (VLPs) that are released from cells (4, 60). The VLPs produced in this manner form a homogeneous population that is morphologically indistinguishable from normal virions. This finding, i.e., that coronavirus assembly does not require the active participation of the nucleocapsid, defined a new mode of virion budding. Furthermore, the coexpression system was used to show that S protein is also dispensable in the assembly process; only the M and E proteins are required for VLP formation (4, 60). This observation accorded well with earlier studies that noted the release of spikeless, noninfectious virions from mouse hepatitis virus (MHV)-infected cells treated with the glycosylation inhibitor tunicamycin (21, 49).

The VLP assembly system has provided a valuable avenue to begin exploring the roles of individual proteins in coronavirus morphogenesis (2, 4, 5, 7, 8, 60), leading to conclusions that, in some cases, have been complemented and extended by the construction of viral mutants (7, 14). One of many critical questions to be resolved is the nature of the apparently passive and optional participation of S protein in the budding process. Clearly, the S protein, although not required for virus assembly, is essential for virus infectivity. Abundant evidence points to the existence of specific interactions between the M and S proteins that are initiated after successful folding of the latter

* Corresponding author. Mailing address: David Axelrod Institute, Wadsworth Center, NYSDOH, New Scotland Ave., P.O. Box 22002, Albany, NY 12201-2002. Phone: (518) 474-1283. Fax: (518) 473-1326. E-mail: masters@wadsworth.org.

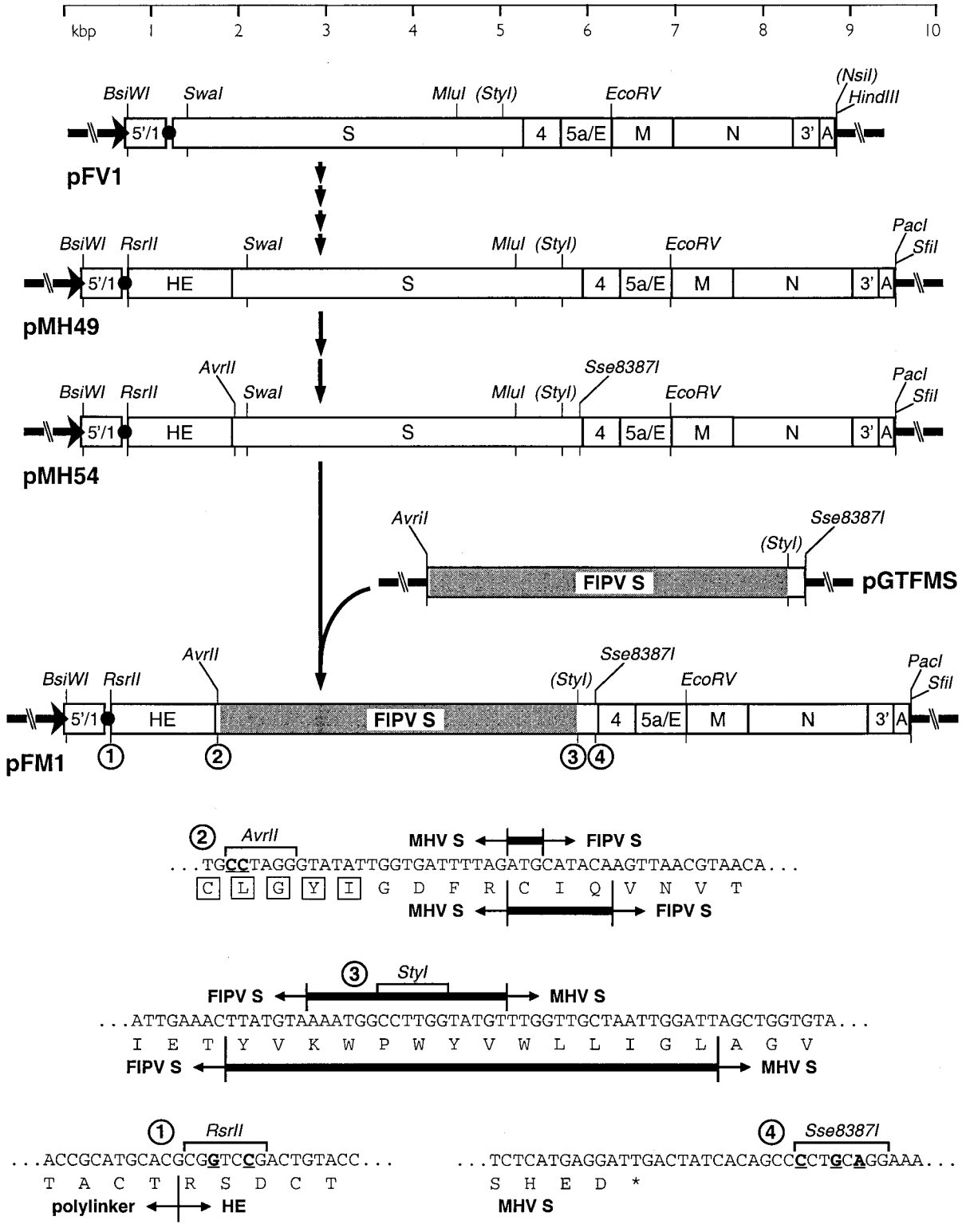

FIG. 1. Construction and composition of the donor RNA template for incorporation of the FIPV S gene ectodomain into MHV. Transcription vector pFM1 was derived from parent plasmid pFV1 (13) via six intermediates, including pMH49 and pMH54, as described in Materials and Methods. The chimeric FIPV-MHV S gene was shuttled into pFM1 from the subclone pGTFMS. MHV and FIPV sequences are indicated, respectively, by open and shaded rectangles. The arrow at the left end of each vector indicates the T7 promoter; the solid circle represents the polylinker between the 5′-end segment of the MHV genome (denoted 5′/1) and the 3′ region containing the structural genes, the 3′ untranslated region (denoted 3′), and the polyadenylated segment (denoted A). Restriction sites relevant to plasmid construction are shown and, unless enclosed in parentheses, are unique in the plasmid in which they appear. At the bottom are shown the sequences in pFM1: 1, between the polylinker and the HE gene fragment; 2, at the MHV-FIPV junction in the signal peptide-encoding portion of the chimeric S gene (with signal peptide residues boxed); 3, at the FIPV-MHV junction in the transmembrane domain-encoding portion of the chimeric S gene; and 4, in the region immediately downstream of the S gene. Nucleotides mutated to create restriction sites are underlined. The boundaries between MHV and FIPV sequence are indicated by short vertical lines; thicker horizontal bars between these indicate nucleotides or amino acids common to both the MHV and FIPV sequences.

in the endoplasmic reticulum (36, 38, 39). S multimers must somehow fit specifically into the interstices of the arrays of M (or M and E) monomers without contributing much to their overall stability.

To investigate which residues of S are involved in this association, VLPs were assembled from components of MHV and feline infectious peritonitis virus (FIPV) (15a). MHV and FIPV belong to two different groups of coronaviruses, and each is highly specific for its corresponding host species. The S proteins of MHV and FIPV, with 1,324 and 1,452 residues, respectively, have only 26% overall amino acid identity, with their greatest divergence occurring in the amino-terminal half of each molecule (6). They recognize different receptors: members of the murine biliary glycoprotein family for MHV (10) and feline aminopeptidase N (fAPN) for FIPV (19, 28, 58). Moreover, the locus of the receptor binding site varies for each, mapping in the amino-terminal 330 residues for the MHV S protein (29) but within amino acids 600 to 676 for the FIPV S protein, by analogy to the highly conserved S protein of porcine transmissible gastroenteritis virus (16). An additional point of difference is that during maturation the MHV S protein is proteolytically cleaved into two moieties of roughly equal size whereas the FIPV S protein remains intact. It was learned from experiments with the coexpression system that while the FIPV S protein could assemble into homologous FIPV VLPs, it could not be incorporated into heterologous VLPs formed by the MHV M and E proteins. By contrast, a chimeric S protein, composed of the entire ectodomain of FIPV S linked to the transmembrane domain and short carboxy-terminal cytoplasmic tail of MHV S, was fully able to be incorporated into MHV VLPs (15a). In addition, the reciprocal construct, having the MHV S ectodomain linked to the FIPV transmembrane domain and cytoplasmic tail, was incorporated into FIPV VLPs. From these results, it could be concluded that the transmembrane and endodomains of a given S protein contain sufficient information for assembly into VLPs of the same species.

It remained to be resolved whether this principle would apply to the complete MHV virion and whether a heterologous S ectodomain in this context would still be functional in receptor binding and membrane fusion. To determine this, we sought to obtain a viable MHV mutant containing the equivalent FIPV-MHV chimeric S protein. Through targeted RNA recombination (13, 27, 35) and selection on cells of the heterologous species, we were able to construct such a recombinant. The resulting chimeric virus (designated fMHV) had the host range characteristics that would be predicted for this type of mutant: it was able to grow in feline cells, and it was no longer able to grow in murine cells. The availability of fMHV is an important first step toward identification of the specific molecular interactions allowing S protein participation in the viral assembly process and toward our understanding of the principles governing viral particle formation.

MATERIALS AND METHODS

Virus, cells, and antibodies. Wild-type MHV-A59 and MHV mutants Alb4, Alb129, and Alb203 (all containing the wild-type MHV S gene) were propagated in mouse 17 clone 1 (17Cl1) cells or Sac(−) cells, and plaque assays and purifications were carried out with mouse L2 cells. Alb4 is a temperature-sensitive N gene deletion mutant which grows optimally at 33°C (27). Alb129, which contains a phenotypically silent marker in gene 4 (13), and Alb203, which contains a phenotypically silent mutation in the M gene (7), were constructed from Alb4 by targeted recombination. MHV was radiolabeled in a cell line derived from L cells transfected with the MHV receptor, designated LR7, which was prepared in the same manner as described previously (45). Selection, propagation, plaque assay, radiolabeling, and neutralization of fMHV and FIPV (strain 79-1146) were done with feline FCWF cells (American Type Culture Collection). mTAL cells are mouse kidney medullary thick ascending limb cells adapted to growth on a plastic support (46). Usage of the fAPN receptor by fMHV was analyzed with MKFA cells, a subline of mTAL cells constitutively expressing the fAPN gene.

Monoclonal antibody (MAb) J1.3 directed against the MHV M protein and MAb WA3.10 against the MHV S protein (15) were provided by J. Fleming (University of Wisconsin, Madison, Wis.). The production of polyclonal antiserum K134 to MHV-A59 has been described previously (47). MAb 23F4.5 was kindly provided by Rhône Mérieux (Lyon, France). This MAb recognizes the S protein of the serotype II feline coronaviruses, to which FIPV strain 79-1146 belongs (37). G73, a serum from an FIPV-infected cat (provided by H. Vennema), was used as a source of polyclonal antibodies to FIPV. MAb R-G-4 directed against fAPN was obtained from T. Hohdatsu (Kitasato University, Towada, Aomori, Japan).

Plasmid constructs. The progenitor for the donor RNA transcription vector used in this study was pFV1 (see Fig. 1), which, as described previously (13), encodes an RNA containing a short 5′ segment of the MHV genome fused via a polylinker to the S gene and all of the 3′ end of the MHV genome thereafter. The region of MHV carried by pFV1 was enlarged in a series of steps that resulted in pMH49 (see Fig. 1), a vector containing most of the upstream HE coding region as well as a new truncation cassette downstream of the poly(A) tail, harboring the unique restriction sites *Pac*I and *Sfi*I. To facilitate replacement of the S gene in pMH49, splicing overlap extension (SOE)-PCR (22) was used twice: (i) to introduce an *Avr*II site into the *Rsr*II-*Swa*I segment (and concomitantly to repair a point mutation generated in a previous PCR step) and (ii) to introduce an *Sse*8387I site into the *Mlu*I-*Eco*RV segment.

The resulting plasmid, pMH54 (see Fig. 1), encodes a T7 RNA polymerase transcript of 9,139 nucleotides (nt) followed by a poly(A) tail of approximately 115 nt. This contains the 5′ 467 nt of the MHV genome (preceded by 2 G nucleotides) fused in frame, through a 72-nt linker, to codon 28 of the HE pseudogene. From that point, its sequence exactly follows the composition of the 3′ end of the wild-type MHV genome except for the following intentional alterations (see Fig. 1): (i) coding-silent changes introduced into codons 28 and 29 of the HE pseudogene, creating an *Rsr*II site; (ii) coding-silent changes introduced into codons 12 and 13 of the S gene, creating an *Avr*II site; (iii) coding-silent changes made originally in pFV1 (13) in codons 173 and 174 of the S gene, eliminating a *Hin*dIII site and creating an *Ase*I site; and (iv) an *Sse*8387I site introduced 12 nt downstream of the S gene stop codon. We also note that in our laboratory strain of MHV-A59, base 2132 of the previously reported gene 2a-HE sequence (34) (GenEMBL accession no. M23256) is not present: TTTT TGAATGTTTT thus becomes TTTTTGATGTTTT. The corrected carboxy terminus of the MHV-A59 HE gene product is consequently longer and is homologous to that of MHV-JHM (54).

In the final vector, a chimeric FIPV-MHV S gene was shuttled into pMH54 from the subclone pGTFMS (Godeke et al., unpublished), into which the *Avr*II and *Sse*8387I sites had been introduced at positions corresponding to those in the MHV S gene construct. The FIPV portion of the chimeric S gene was identical to that reported by de Groot et al. (6) (GenEMBL accession no. X06170). The resulting plasmid was designated pFM1 (see Fig. 1).

Manipulations of DNA were carried out by standard methods (50). The compositions of all constructs were checked by restriction analysis; all cloned cDNA precursors, PCR-generated segments, and newly created junctions of each plasmid were verified by DNA sequencing by the method of Sanger et al. (51) with modified T7 DNA polymerase (Sequenase; U.S. Biochemicals) or by automated sequencing with an Applied Biosystems 373A or 377 DNA sequencer.

Targeted recombination. A chimeric FIPV-MHV S gene was transduced into the MHV genome by targeted RNA recombination between pFM1-generated donor RNA and the recipient virus, Alb4, essentially as described previously (13, 35). Capped, runoff donor transcripts were synthesized from *Pac*I-truncated pFM1 with a T7 RNA polymerase kit (Ambion) as specified by the manufacturer. Donor RNA, without further purification, was transfected into Alb4-infected L2 spinner culture cells, following a 2-h infection at 33°C, by using two pulses at 960 μF and 0.3 kV in a Gene Pulser electroporation apparatus (Bio-Rad). Infected and transfected cells were then plated onto monolayers of FCWF cells. At 24 to 72 h after infection at 33°C, when syncytia could be detected in the FCWF monolayers, progeny virus in the supernatant medium were harvested and candidate recombinants were purified by two rounds of plaque titer determination on FCWF cells at 37°C. Side-by-side controls, originating from Alb4-infected L2 cells that had been mock transfected or transfected with RNA from the parent vector pMH54, were treated identically.

Genomic analysis of candidate recombinants. Independently isolated and purified plaques of fMHV were used to infect 25-cm^2 monolayers of FCWF cells at 37°C, and total cellular RNA was harvested at 24 to 30 h postinfection and purified either by a Nonidet P-40 gentle-lysis method (25) or with Ultraspec reagent (Biotecx). Control RNA samples were purified from MHV-infected 17Cl1 cell monolayers. RNA was reverse transcribed under standard conditions (50) with a random primer, $p(dN)_6$ (Boehringer Mannheim), and cDNA was amplified by PCR with various primer pairs to characterize candidate recombinants. PCR amplifications were run for 30 cycles of 1 min at 94°C, 1 min at 48°C, and 2 min at 72°C with AmpliTaq DNA polymerase (Perkin-Elmer), except for PCR amplifications of the entire S gene, which were carried out with r*Tth* DNA polymerase (Perkin-Elmer) for 30 cycles of 30 s at 94°C, 1 min at 50°C, and 10 min at 68°C. Products were directly analyzed by agarose gel electrophoresis or were gel purified prior to restriction digestion and analytical gel electrophoresis.

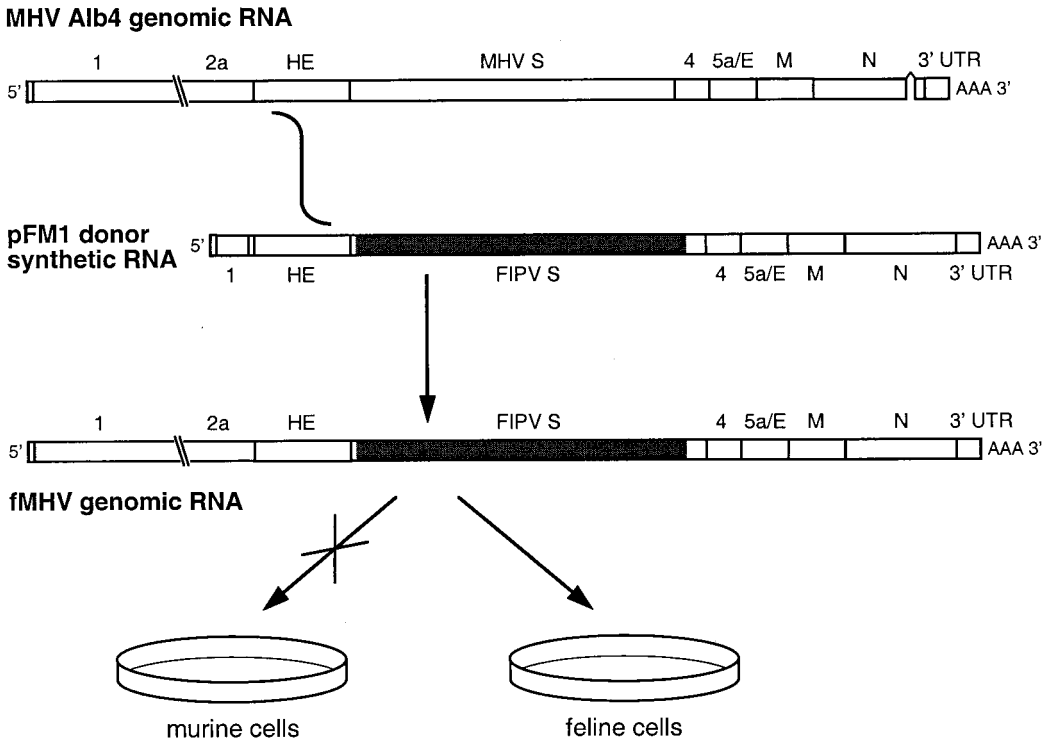

FIG. 2. Scheme for construction of fMHV by targeted recombination between the MHV N gene deletion mutant, Alb4 (27), and donor RNA transcribed from the plasmid pFM1. The deletion in the Alb4 N gene is shown as a discontinuity. A single crossover event anywhere within the HE gene fragment of the donor RNA should generate a recombinant, fMHV, containing both the ectodomain-encoding region of the FIPV S gene (shaded) and the wild-type MHV N gene. The recombinant should simultaneously lose the ability to infect murine cells and gain the ability to infect feline cells.

Direct RNA sequencing was performed by a modified dideoxy termination method (11, 40).

Intracellular viral protein analysis. LR7 cells and FCWF cells were grown in 35-mm dishes and infected with MHV-A59, fMHV, or FIPV at a multiplicity of 10 PFU per cell. Before being labeled, the cells were starved for 30 min in cysteine- and methionine-free minimal essential medium containing 10 mM HEPES (pH 7.2) without fetal bovine serum. The medium was then replaced by 600 μl of the same medium containing 100 μCi of ^{35}S in vitro cell-labeling mix (Amersham) and, for FCWF cells, 25 μCi of [^{35}S]cysteine (ICN). MHV-A59-infected LR7 cells were labeled from 5 to 6 h postinfection, and fMHV- and FIPV-infected FCWF cells were labeled from 7 to 8 h postinfection. After the labeling period, the cells were washed with phosphate-buffered saline (PBS) and solubilized in 1 ml of lysis buffer, consisting of TES (20 mM Tris HCl [pH 7.5], 100 mM NaCl, 1 mM EDTA) containing 1% Triton X-100 and 2 mM phenylmethylsulfonyl fluoride. Nuclei were removed from the cell lysates by centrifugation at 12,000 × *g* for 10 min at 4°C.

For immunoprecipitations, 50-μl aliquots of lysate were diluted with 1 ml of detergent solution (50 mM Tris HCl [pH 8.0], 62.5 mM EDTA, 0.5% Nonidet P-40, 0.5% sodium deoxycholate) and 30 μl of 10% sodium dodecyl sulfate (SDS) was added. Antibodies were then added: 3 μl of antiserum K134, 10 μl of MAb WA3.10, 3 μl of serum G73, or 3 μl of MAb 23F4.5. After an overnight incubation at 4°C, immune complexes were adsorbed for 1 h to formalin-fixed *Staphylococcus aureus* cells (BRL Life Technologies) added as 45 μl of a 10% (wt/vol) suspension. Immune complexes were collected by centrifugation at 12,000 × *g* and washed three times with RIPA buffer (20 mM Tris HCl [pH 7.5], 150 mM NaCl, 5 mM EDTA, 1% Triton X-100, 0.1% SDS, 1% sodium deoxycholate). Pellets were resuspended in 30 μl of Laemmli sample buffer (30) and were heated for 2.5 min at 95°C or, where indicated, were kept at room temperature. Samples were analyzed by electrophoresis in an SDS–12.5% polyacrylamide gel followed by fluorography.

Labeling, purification, and analysis of virion proteins. Cells were infected and labeled as described above, except that labeling periods were from 6 to 9 h postinfection for LR7 cells or from 7 to 10 h postinfection for FCWF cells. At the end of the labeling period, culture media (0.8 ml) were collected, cleared by low-speed centrifugation, mixed with 2.3 ml of 67% sucrose in TM (10 mM Tris HCl [pH 7.0], 10 mM $MgCl_2$), and transferred into Beckman SW50.1 ultracentrifuge tubes. Each solution was overlaid with 1 ml of 48% sucrose, 0.5 ml of 40% sucrose, and 0.5 ml of 30% sucrose in TM, and the gradients were centrifuged at 155,000 × *g* (36,000 rpm) for 43 h. After centrifugation, a fraction consisting of the top 1 ml of each tube was collected. Virus particles were affinity purified from 150 μl of this fraction by addition of 25 μl of MAb J1.3, 3 μl of MAb WA3.10, 3 μl of serum G73, or 3 μl of MAb 23F4.5. Samples were processed and analyzed as above, except that the *S. aureus* immune complexes were washed once with TM instead of three times with RIPA buffer.

Neutralization of viral infectivity. Comparable amounts of infectivity (10^5 PFU) of MHV, fMHV, or FIPV were incubated for 1 h at 37°C in 100 μl of PBS–DEAE to which was added 3 μl of polyclonal antibody K134 or 3 μl of serum G73. The viruses were inoculated onto LR7 cells (MHV-A59) or FCWF cells (fMHV and FIPV) grown on coverslips in 35-mm culture dishes. After 1 h, the cells were washed and incubated in culture medium. At 6 h postinfection, the cells were rinsed once with PBS and fixed with precooled (−20°C) methanol for 10 min at −20°C. The cells were washed three times with PBS and incubated with antibody K134 (1:300) or with serum G73 (1:200). After 30 min at room temperature, the cells were rinsed three times with PBS and stained with fluorescein isothiocyanate-conjugated or tetramethylrhodamine isothiocyanate-conjugated goat anti-rabbit or goat anti-cat immunoglobulin G antibody (Cappel), both diluted in PBS (1:200). Finally, the cells were washed three times with PBS and mounted in FluorSave reagent (Calbiochem). Fluorescence was viewed with a Leica TCS4D confocal laser-scanning microscope.

Inhibition of infection by antireceptor antibodies. MKFA cells grown on glass coverslips in 35-mm culture dishes were preincubated for 1 h at 37°C with undiluted MAb R-G-4 against the feline receptor (20) or with culture medium as a control. They were then infected with MHV, fMHV, or FIPV at a multiplicity of 5 PFU per cell as described above. At 6 h (MHV, fMHV) or 7 h postinfection (FIPV), the cells were fixed and stained as described above with antibody K134 (MHV, fMHV) or serum G73 (FIPV) and, as second antibodies, fluorescein isothiocyanate-conjugated goat anti-rabbit or goat anti-cat immunoglobulin G antibodies.

RESULTS

Generation of an MHV mutant carrying a chimeric FIPV-MHV S gene. In previous work, we and others have created site-directed point mutations in the MHV S gene by targeted recombination with donor RNAs derived from pFV1 (13, 32). This transcription vector contains the 3′-most 7.4 kb of the MHV genome, which consists of all sequence distal to the start of the S gene (Fig. 1). For the present work, in which we sought

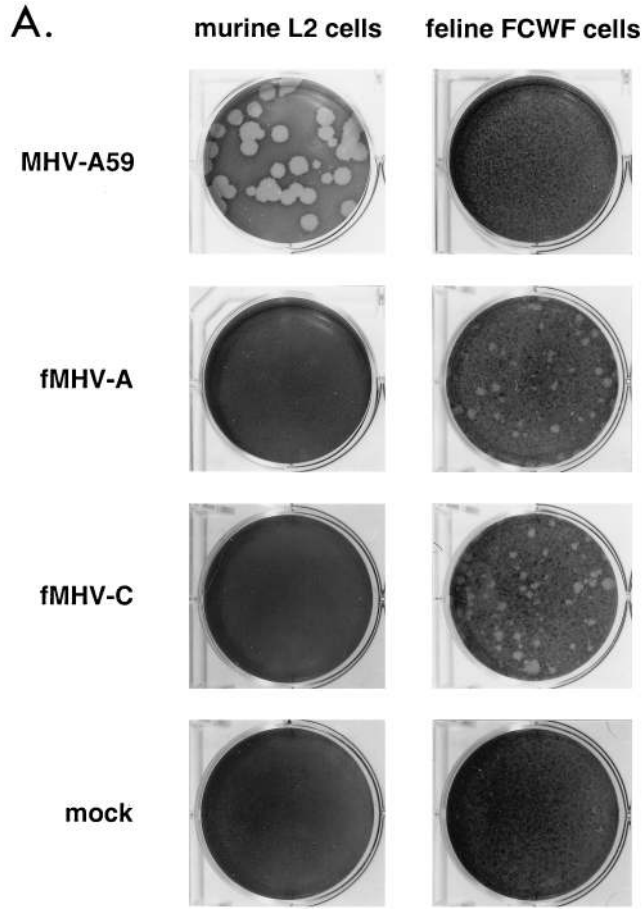

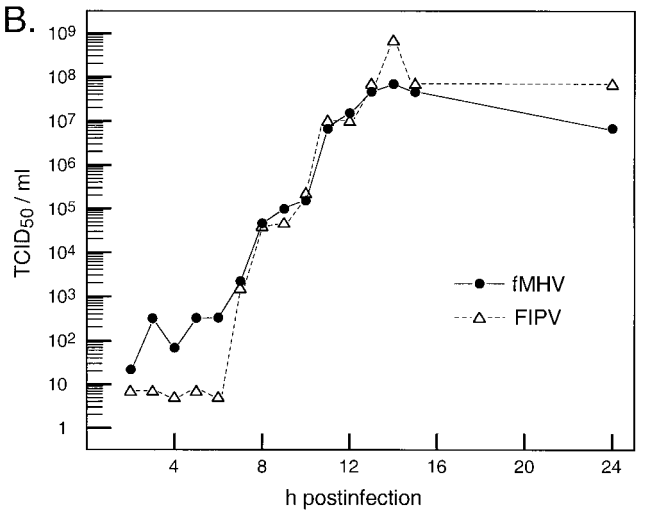

FIG. 3. Growth of fMHV in feline cells. (A) Plaque-forming ability of fMHV. Monolayers of murine L2 cells or feline FCWF cells were mock infected or infected with wild-type MHV or either of two independent isolates of fMHV. Plaques were visualized at 66 h postinfection, after staining with neutral red. (B) Single-step growth kinetics of fMHV-C and FIPV in FCWF cells. Viral infectivity in culture medium at different times postinfection was determined by a quantal assay on FCWF cells, and 50% tissue culture infective doses ($TCID_{50}$) were calculated.

to completely replace the S gene, we constructed a larger vector to provide sufficient material flanking the 5′ end of the gene to enhance the probability of upstream homologous crossover events between the donor RNA and the genome of the recipient virus. The resulting enlarged vector, pMH54, contained almost all (1.2 kb) of the upstream HE pseudogene as well as two unique restriction sites that were inserted to facilitate the exchange of S gene variants (Fig. 1, sequences 2 and 4). The first of these, *Avr*II, was generated by two coding-silent nucleotide changes in the 5′-proximal portion of the S gene, which encodes the signal peptide. The second, *Sse*8387I, was created by base changes 12, 15, and 17 nt downstream of the stop codon of S. Both sites were expected to be phenotypically silent when introduced into the MHV genome, an assumption which later proved correct (42; L. Kuo and P. S. Masters, unpublished results).

A chimeric FIPV-MHV S gene was then incorporated into pMH54 from pGTFMS, producing the vector pFM1 (Fig. 1). In the chimeric S gene, the principal point of exchange was at a *Sty*I site falling within the region encoding a 14-amino-acid stretch, YVKWPWYVWLLIGL, that borders the transmembrane domain and is common to both S proteins (Fig. 1, sequence 3). The choice of this locus, which constitutes the largest continuous segment of amino acid identity between the MHV and FIPV sequences, was predicated on expression system results that demonstrated that swapping of S protein ectodomains here allowed incorporation of the chimeric S protein into MHV VLPs (15a). A secondary MHV-FIPV junction was designed within a 3-amino-acid motif, CIQ, that is common to both S proteins and follows the signal peptide of each by 5 or 6 residues (Fig. 1, sequence 2). This was done to preserve the MHV genomic region of some 70 nt immediately downstream of the intergenic sequence preceding the S gene, in case this influenced the transcription efficiency of the S mRNA. Thus, in the mature chimeric S molecule, the entire ectodomain of the MHV S protein would be replaced by the entire ectodomain of the FIPV S protein, except for replacement of the first five residues of FIPV S with the first four residues of MHV S.

TABLE 1. Primers used for RT-PCR analysis of fMHV

Primer	Gene	Sense	Sequence
LK68	FIPV S	−	5′TTCTTGTGCTGCTACACC3′
FF29	HE	+	5′TTTTATGACGGATAGCGG3′
LK56	FIPV S	+	5′AGGCTAGACTTAATTATG3′
PM252	Gene 4	−	5′GCCAGGTAGCAATGAGAA3′
FF50	MHV S	−	5′TTATGGTTGTTTATGGTG3′
PM232	MHV S	+	5′GATGTATCCAGCTTGTGA3′
LK71	Gene 2a	+	5′ACCGTGTGTAGAATGAAGGGTTGTATG3′
CK1	MHV S	−	5′ACCGGGTAGTAACCAGTA3′
LK69	FIPV S	−	5′GTCATCATTCCACTCAAG3′

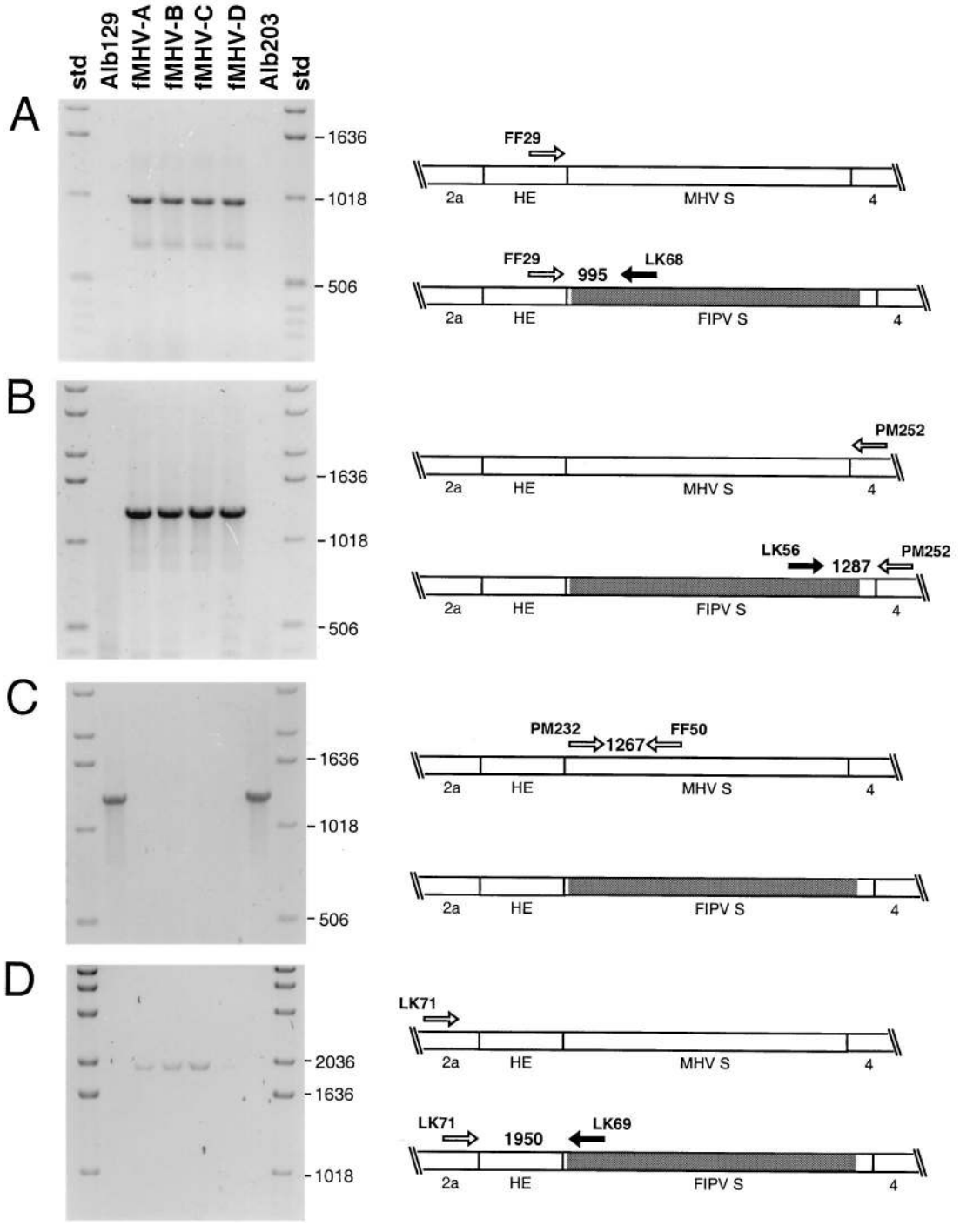

FIG. 4. PCR analysis of fMHV recombinants. In each experiment, RT-PCR was used to amplify regions of RNA isolated from cells infected with each of four independent isolates of fMHV or two MHV controls. The controls, Alb129 (13) and Alb203 (7), are MHV mutants that were also obtained by targeted recombination between Alb4 and pFV1-related donor RNAs; both are phenotypically wild type and are isogenic with wild-type MHV in the region under analysis. PCR products were analyzed by electrophoresis in 0.8% agarose gels stained with ethidium bromide. Sizes of relevant standard (std) marker DNA fragments are indicated on the right or left of each gel. PCR primers (Table 1) used in each experiment, their loci in the MHV or fMHV genomes, and the predicted sizes of the PCR products or restriction fragments of the PCR products are indicated on the right.

Donor RNA transcribed in vitro from pFM1, or from pMH54 as a control, was transfected into mouse L2 cells that had been infected with the thermolabile MHV N gene deletion mutant Alb4 (27). Infected and transfected cells were then overlaid onto monolayers of feline FCWF cells to select for recombinants that, as a result of a crossover upstream of the S genes of donor and recipient RNAs, had acquired the ability to infect feline cells and simultaneously had lost the ability to infect murine cells (Fig. 2). All FCWF monolayers that had received pFM1 RNA-transfected, Alb4-infected L2 cells un-

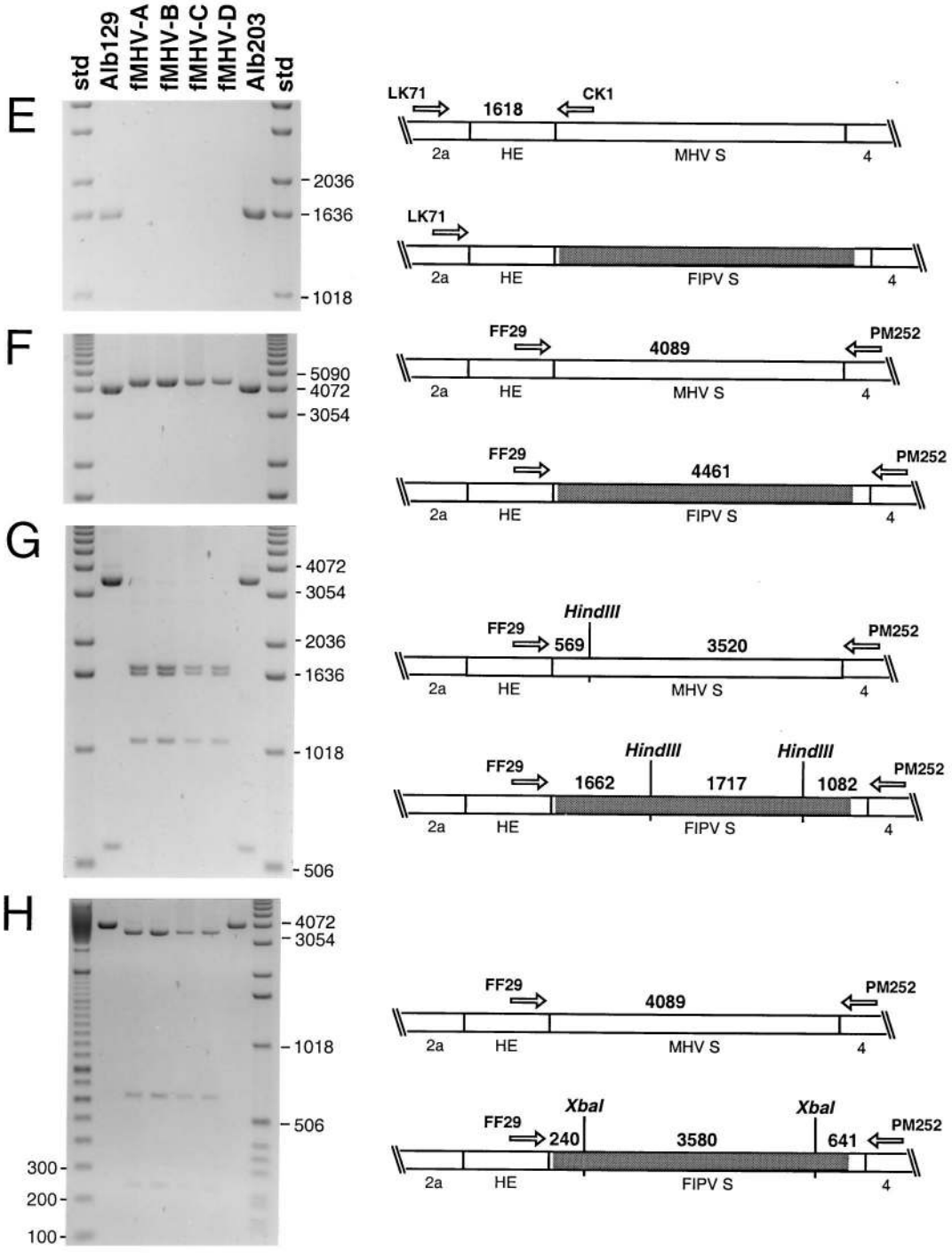

FIG. 4—*Continued.*

equivocally exhibited syncytium formation by 48 h postinfection. By contrast, FCWF monolayers that had received mock-transfected or pMH54 RNA-transfected, Alb4-infected L2 cells showed no detectable syncytia by 96 h postinfection.

Supernatant media from these infected and transfected cells were harvested, clarified by centrifugation, and used in plaque titer determinations on FCWF cells. At 48 and 72 h postinfection, plaques were clearly observed for samples derived from pFM1 RNA whereas no detectable plaques were obtained from samples that had been mock transfected or transfected with pMH54 RNA. Plaques of four independent candidate recombinants derived from four separate transfections, designated fMHV-A, fMHV-B, fMHV-C, and fMHV-D, were purified and analyzed further.

Tissue culture growth phenotype of fMHV. Consistent with prediction, all four fMHV recombinants were unable to produce syncytia or cytopathic effects in murine 17Cl1 cells or to give rise to plaques in murine L2 cells. As shown in Fig. 3A, no

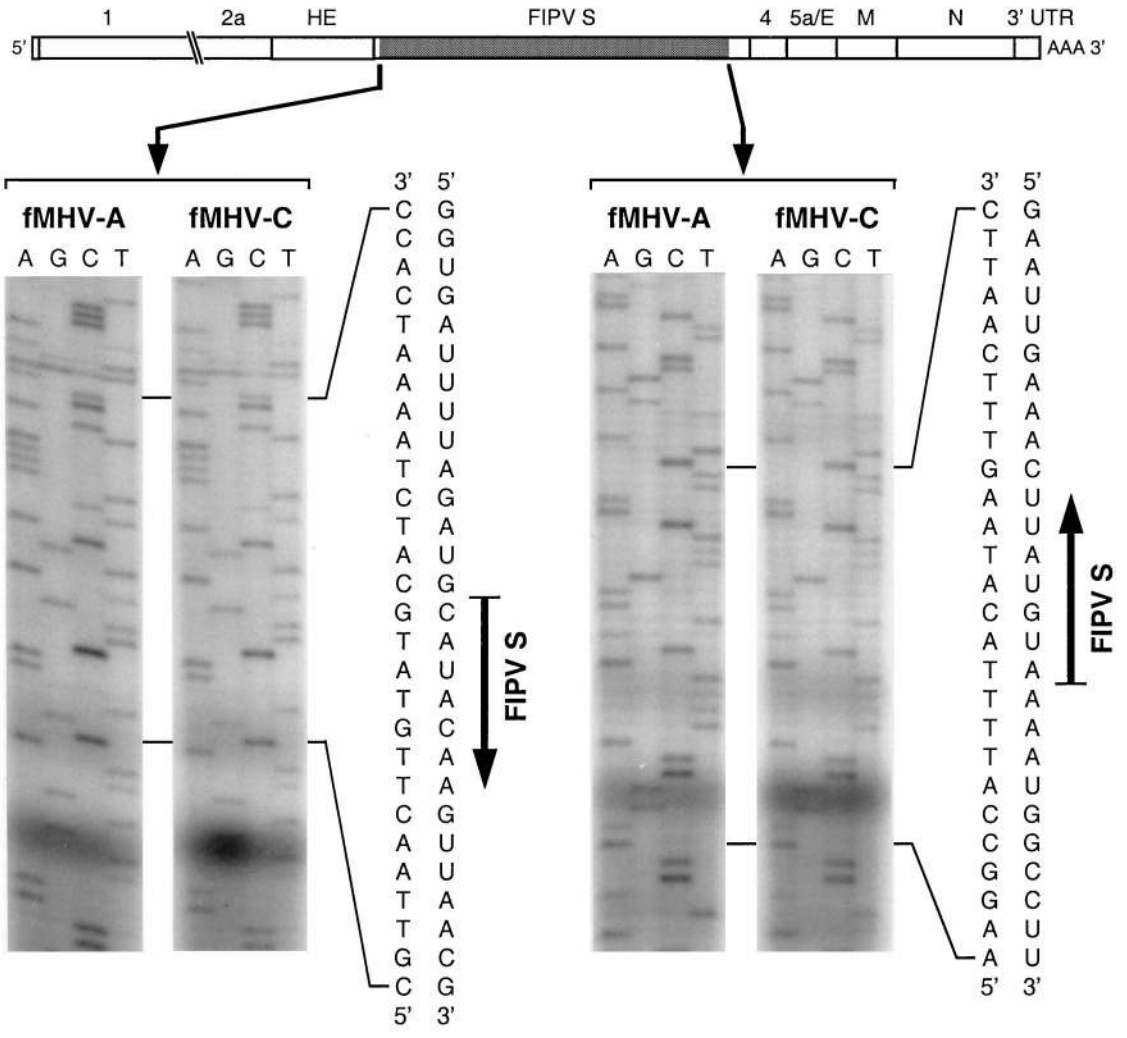

FIG. 5. RNA sequence of the FIPV-MHV S gene junctions in fMHV. RNA isolated from cells infected with independent recombinants fMHV-A and fMHV-C was sequenced with a primer complementary to nt 118 to 141 of the FIPV S gene (left set, upstream junction) or a primer complementary to nt 3817 to 3837 of the MHV S gene (right set, downstream junction). For each junction, both the directly read negative-strand cDNA sequence and the inferred positive-strand RNA sequence are shown.

plaques of any size were evident on L2 cell monolayers by 66 h following inoculation with fMHV-A or fMHV-C, in contrast to the large, clear plaques generated by wild-type MHV on the same cells. Conversely, at the same time postinfection, smaller plaques were obvious on FCWF monolayers infected with the fMHV isolates but wild-type MHV was absolutely unable to form plaques on these cells. This result confirmed the expectation that the replacement of the MHV S protein with the chimeric FIPV-MHV S protein completely switched the host species specificity of the virus. The data shown in Fig. 3A were intentionally obtained in a laboratory that has never held FIPV, to preclude the possibility of cross-contamination.

The fMHV recombinants grew efficiently in FCWF cells, exhibited similar growth kinetics to FIPV (Fig. 3B), and caused extensive syncytia and cytopathic effect comparable to that caused by FIPV. Stocks of the recombinant virus typically reached titers an order of magnitude lower than the titers obtained with FIPV. Thus, exchange of the S protein ectodomain was sufficient to allow complete crossing of the host cell species barrier by fMHV. However, this chimeric recombinant was not entirely as fit as FIPV in its ability to grow in tissue culture. Possible reasons for this observation are discussed below.

Genomic analysis of fMHV. To ascertain the genomic structure of the fMHV candidates, we purified RNA from feline cells infected with four independent isolates of the recombinant as well as from murine cells infected with MHV controls. Multiple sets of random-primed reverse transcription followed by PCR (RT-PCR) were performed with the primers listed in Table 1. First, to determine whether the engineered FIPV-MHV S gene boundaries were indeed present in the recombinants, primers specific for FIPV S gene regions near both the 5′ and 3′ junctions were used together with MHV-specific primers positioned on the opposite side of each junction. At the 5′ junction, when the FIPV S-specific primer LK68 was paired with the MHV HE-specific primer FF29, a PCR product consistent with the expected size of 995 bp was generated only from the fMHV isolates but not from the MHV controls (Fig. 4A). Similarly, primers LK56 and PM252, flanking the 3′ FIPV-MHV junction, generated an apparent 1,287-bp product from fMHV but not from the MHV controls (Fig. 4B). To ensure that the lack of signal from the control MHV strains,

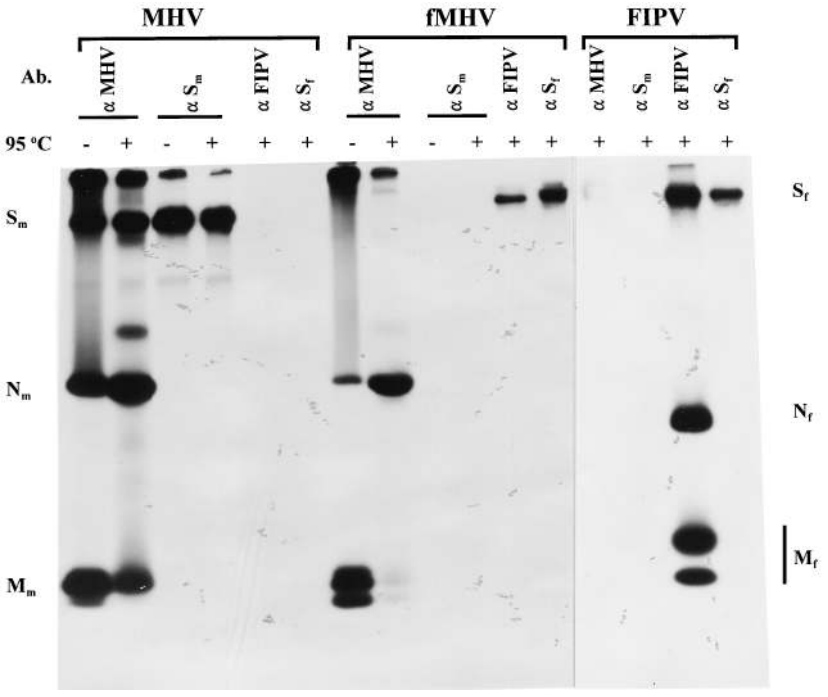

FIG. 6. Viral proteins in fMHV-infected cells. FCWF cells infected with fMHV and, for comparison, FIPV-infected FCWF cells and MHV-infected LR7 cells were labeled for 1 h with ^{35}S-amino acids. Immunoprecipitations were performed on aliquots of cleared lysates of these cells by using the following antibodies (Ab.): K134 rabbit serum against purified MHV-A59 (αMHV); serum G73 from a FIPV-infected cat (αFIPV); and MAb WA3.10 and 23F4.5, recognizing the ectodomains of MHV S (αS_m) and FIPV S (αS_f), respectively. As indicated, proteins were heated at 95°C (+) or analyzed without heating (−) in SDS–12.5% polyacrylamide gels. The positions of the S, M, and N proteins in the gel are indicated on the left for MHV and on the right for FIPV.

Alb129 and Alb203, was not due to failure of the RT-PCR, RNA samples were analyzed with a set of MHV S-specific primers, PM232 and FF50. This produced a PCR fragment of 1,267 bp only for the MHV controls but not for the fMHV isolates (Fig. 4C). This result not only verified the specific presence of FIPV S sequences in the fMHV isolates but also indicated that they were devoid of any residual presence of the Alb4 parent.

To rule out the possibility that FIPV S-specific RT-PCR products were actually amplified from input pFM1 donor RNA that had somehow persisted through plaque purification and passaging, a gene 2a-specific primer, LK71, was paired with the FIPV S-specific primer LK69. This yielded a 1,950-bp product from fMHV RNA (and not from control MHV RNA) (Fig. 4D), which could not have originated from pFM1 RNA since the latter does not contain any gene 2a sequence (Fig. 1). This finding, together with the absence of any detectable MHV S-specific signal from fMHV RNA, indicated that the FIPV S gene segment was indeed in the context of a recombinant genome. In an additional control, the specificity of primer LK71 was demonstrated by pairing it with the MHV S-specific primer CK1, which produced a product consistent with the expected size of 1,618 bp only with the MHV samples (Fig. 4E).

It seemed unlikely that additional homologous crossovers could have occurred within the ectodomains of the MHV and the chimeric S genes of the recipient and donor RNAs, owing to the low degree of sequence homology between the two. However, this possibility could not be excluded on the basis of the above data. Therefore, to examine whether the whole chimeric S gene was present in the recombinants, the upstream HE-specific primer FF29 and the downstream gene 4-specific primer PM252 were used to amplify the entire S gene region of

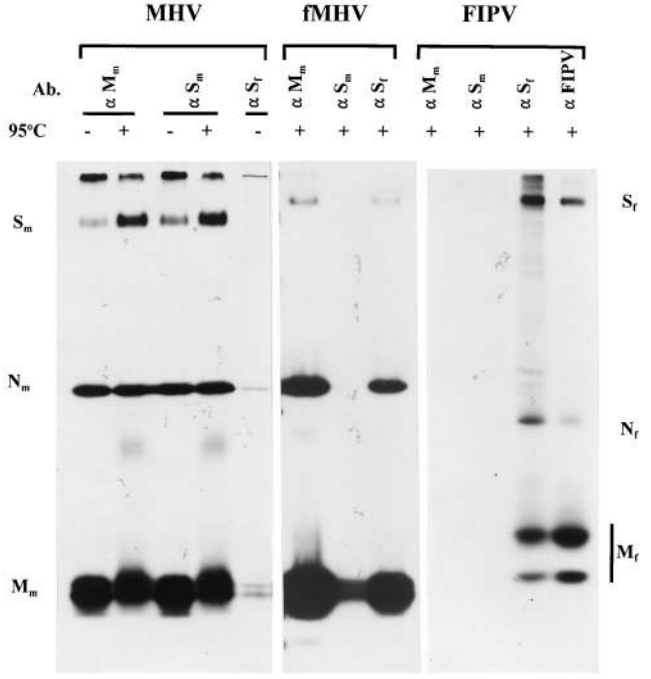

FIG. 7. Protein composition of purified fMHV. ^{35}S-labeled fMHV and, for comparison, similarly labeled FIPV and MHV were prepared and purified by floatation in sucrose gradients. Virus particles were subsequently affinity purified with specific antibodies and analyzed in an SDS–12.5% polyacrylamide gel. Indications are as described in the legend to Fig. 6.

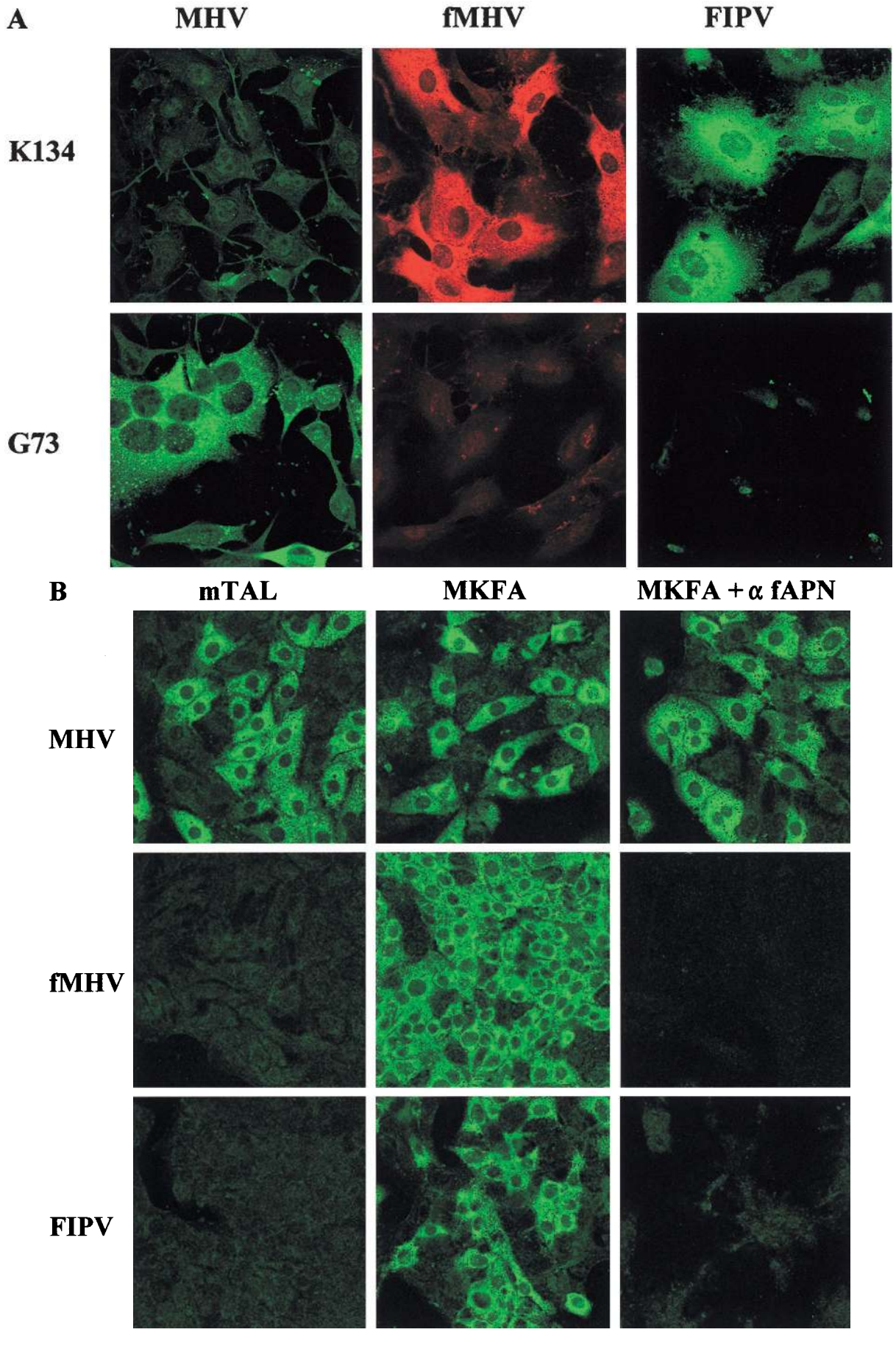
A
MHV
fMHV
FIPV
K134
G73
B
mTAL
MKFA
MKFA + α fAPN
MHV
fMHV
FIPV

the fMHV isolates and MHV controls. This gave a single PCR product consistent with the expected size of 4,089 bp for MHV and a larger single product, predicted to be 4,461 bp, for fMHV (Fig. 4F). Moreover, digestion of these products with *Hin*dIII (Fig. 4G), *Xba*I (Fig. 4H), or *Spe*I (data not shown) yielded exactly the predicted sets of restriction fragments for all the fMHV isolates and the MHV controls. Since these enzymes differentially cleave the MHV S gene and the chimeric S gene at intervals spanning their entire lengths, we concluded that each fMHV strain contained the unaltered chimeric FIPV-MHV S gene.

An additional RT-PCR, with primers flanking the locus of the 87-nt deletion in the N gene in Alb4, as described previously (27, 40), revealed that all four independent fMHV isolates contained the wild-type N gene (data not shown). The acquisition of this marker, 2.9 kb distant from the S gene and only 0.4 kb from the 3′ end of the genome, supports the notion that each of the fMHV mutants was generated by a single crossover, as depicted in Fig. 2.

To further verify the presence of the chimeric S gene in the recombinants, we directly sequenced the FIPV-MHV junctions in RNA isolated from FCWF cells infected with fMHV-A or fMHV-C. At both the upstream and the downstream boundaries, both recombinants exhibited the expected transition between MHV S sequence and FIPV S sequence (Fig. 5). In addition, the RNA sequence of the 5′ end of the HE genes of fMHV-A and fMHV-C revealed that no heterologous region of the pFM1 RNA polylinker had been introduced by a possible nonhomologous recombination event (data not shown). Since all the available evidence suggested that the independent isolates of fMHV were identical, a single isolate, fMHV-C, was used for all subsequent analyses.

As a final confirmation of the composition of fMHV-C, we directly sequenced RT-PCR products encompassing the entire S gene of this virus. These products were obtained in the same manner as those shown in Fig. 4, except that specific, rather than random, primers were used for the RT step. This analysis showed that the sequence of fMHV-C, from the end of the HE gene through the start of gene 4, including both the FIPV and MHV portions of the chimeric S gene, was identical to that of plasmid pFM1, from which donor RNA had been transcribed. This result ruled out the possibility that, in isolating fMHV, we had inadvertently selected for additional mutations in the S gene that may have contributed to the assembly or infectivity of this virus.

Analysis of viral proteins in fMHV-infected cells. To characterize the recombinant fMHV at the protein level, in particular with respect to its S protein, we first analyzed the viral polypeptides in infected cells. To this end, we infected FCWF cells with fMHV and labeled the proteins for 1 h with ^{35}S-amino acids. As controls, we infected FCWF and L cells in parallel with FIPV and MHV, respectively, and labeled them similarly. At the end of the labeling period, cell lysates were prepared and immunoprecipitations were carried out with the following antibodies: K134, a rabbit serum raised against purified MHV; G73, a serum from an FIPV-infected cat; WA3.10, a MAb against an epitope present in the MHV S ectodomain (S_m); and 23F4.5, a MAb recognizing an epitope in the FIPV S ectodomain (S_f). Before analysis by SDS-polyacrylamide gel electrophoresis, the immunoprecipitates were briefly heated, except for samples containing the MHV M protein, which were also analyzed unheated in view of the known aggregation of this protein at higher temperatures (56). The electrophoretic patterns are shown in Fig. 6. As expected, the anti-MHV serum did not recognize any proteins in FIPV-infected cell lysates but precipitated the major structural proteins M, N, and S from lysates of MHV-infected cells. The same proteins were detected in the lysates from fMHV-infected cells, except for the S protein, which was clearly absent. This result was confirmed with the anti-S_m antibodies, which recognized the S protein from MHV-infected cells but nothing in the fMHV lysates. In contrast, both the anti-FIPV serum and the anti-S_f MAb precipitated a protein that was significantly larger than MHV S but comigrated with the FIPV S protein, which these antibodies recognized in the FIPV-infected cell lysate. These results indicate that a polypeptide with the expected characteristics of the FIPV-MHV chimeric S protein, 1 residue shorter than the mature FIPV S protein and 124 residues longer than the mature MHV S protein, was synthesized in cells infected with fMHV.

Analysis of fMHV structural proteins. The protein composition of fMHV virions was investigated and compared with those of MHV and FIPV. Proteins synthesized in infected cells were labeled for 3 h with ^{35}S-amino acids, and viral particles released into the culture medium were purified by floatation in sucrose gradients. Virions were subsequently affinity purified by using the anti-FIPV, anti-S_m, and anti-S_f antibodies described above, as well as MAb J1.3, which recognizes an epitope in the MHV M protein ectodomain (7). The fMHV proteins isolated with this last antibody were the MHV M and N proteins and a protein distinctly larger than MHV S but similar in electrophoretic mobility to the FIPV S protein (Fig. 7). No fMHV particles were selected with the anti-S_m MAb, indicating that they did not display the MHV S epitope. They did, however, carry the FIPV S epitope, since the anti-S_f MAb was able to select fMHV virions. These observations are consistent with fMHV virions having the protein composition of MHV, except with spikes composed only of the chimeric FIPV-MHV S protein.

Neutralization of fMHV by anti-FIPV but not by anti-MHV serum. The chimeric virus was further characterized by studying its sensitivity to neutralization of infectivity by MHV- and FIPV-specific antibodies. To this end, fMHV was incubated with antibodies before being inoculated onto FCWF cells. In parallel, samples of FIPV and MHV were treated similarly and used for inoculation of FCWF and LR7 cells, respectively. The effects of antibody pretreatment were evaluated by analyzing the extent of infection through visualization of infected cells in an immunofluorescence assay. Figure 8A shows that fMHV was neutralized efficiently by G73, a serum obtained from an FIPV-infected cat, but not by K134, a rabbit serum raised against purified MHV-A59. This established that FIPV-specific epitopes are exposed on the exterior of fMHV virions.

fAPN receptor-dependence of fMHV infection. To confirm the switch in receptor usage of fMHV as a result of the functional presence of the FIPV spike ectodomain, we made use of a mouse cell line, mTAL (46). These cells are susceptible to MHV but cannot be infected by FIPV. As shown in the im-

FIG. 8. Blocking of spike-receptor interactions. (A) Neutralization of viral infectivity. fMHV, FIPV, and MHV were preincubated with anti-MHV serum (K134) or anti-FIPV serum (G73) before being inoculated on LR7 (MHV) or FCWF cells (fMHV and FIPV). Infection was visualized at 6 h postinfection by immunofluorescence microscopy. (B) Receptor dependence of infection. mTAL and MKFA cells (mTAL cells expressing fAPN), the latter without or with treatment with antibodies to the fAPN receptor, were inoculated with fMHV, MHV, and FIPV, and infection was visualized by immunofluorescence analysis.

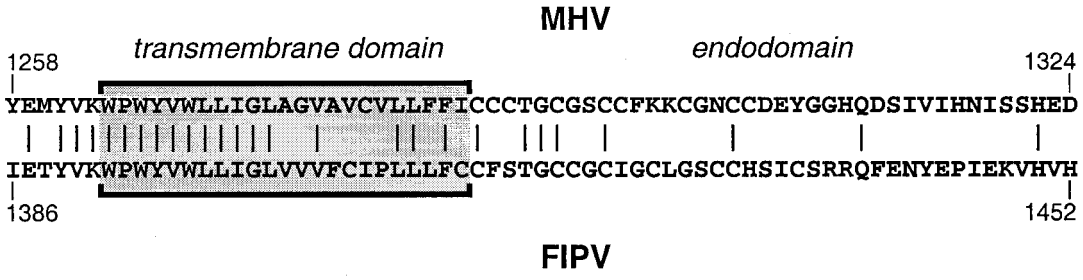

FIG. 9. Amino acid sequence alignment of the carboxy-terminal ends of the MHV and FIPV S proteins.

munofluorescence analysis of Fig. 8B, these cells were also resistant to fMHV. However, MKFA cells, which are mTAL cells that constitutively express the fAPN receptor gene, were found to be susceptible to fMHV infection (Fig. 8B). Moreover, that this infection was indeed mediated by the fAPN protein was corroborated further by the observation that infection of MKFA cells could be blocked by their preincubation with antibodies to the fAPN molecule. These results demonstrated that fMHV cannot use the MHV receptor present on these cells but can enter the cells by binding the FIPV receptor fAPN.

DISCUSSION

Incorporation of S protein into coronaviruses. This study was initiated to localize the portion of the MHV S protein governing its incorporation into mature virions. Although coronavirus assembly can occur independently of S protein (4, 21, 49, 60), this constituent is obviously pivotal to the biology of the virus. It will thus be important to understand the basis of its selective inclusion into particles, and, conversely, the reason why other proteins are excluded. It has been previously shown that there are specific associations between the M and S proteins while M is coalescing into higher-order arrays, and these may be key to recruiting S into budding viral particles (36, 38, 39). However, much remains to be learned of the molecular details of this process, and an active role for E protein cannot be ruled out.

In the work presented here, we were able replace the MHV S ectodomain with that of FIPV, a representative of another of the three groups within the coronavirus genus. The MHV and FIPV S proteins, although ancestrally related, have diverged to the point where there is less than 16% sequence identity between the amino-terminal half of each molecule, and they have evolved to recognize different receptors with different regions of their ectodomains. We have shown that the resulting ectodomain-switched recombinant, fMHV, underwent a corresponding switch of its host cell species specificity. Moreover, it was clear that the chimeric FIPV-MHV S gene had replaced its purely MHV counterpart in the viral genome and that the chimeric S protein product was expressed in infected cells and was incorporated into virions. It should be noted that both genomic analysis and immunochemistry demonstrated that only the chimeric S gene was present and only the chimeric S protein was expressed in fMHV-infected cells and fMHV virions. Therefore, the altered host cell specificity was not the result of phenotypic mixing of the MHV genome packaged into particles containing the FIPV-MHV S chimera expressed from donor RNA.

The rationale for the ectodomain substitution that was made in fMHV was derived from a more comprehensive series of chimeric gene expression experiments involving the VLP assembly system (15a). We have previously constructed MHV mutants by targeted recombination to extend the results of VLP experiments that established the critical role of the carboxy-terminal extremity of the M protein in virion formation (7). The combined power of the two approaches has enabled us to examine mutations of essential structural genes in order to probe molecular interactions central to coronavirus assembly. In the present work, incorporation of the chimeric FIPV-MHV S protein into fMHV delimits the region of S required for inclusion into the virion envelope to the carboxy-terminal 64 of its 1,324 amino acid residues (Fig. 9). Common features between the FIPV and MHV S proteins, a conserved transmembrane domain and a cysteine-rich endodomain, were not sufficient for FIPV S protein to be taken up into assembled VLPs formed by the MHV M and E proteins. Therefore, further experiments will now be aimed toward determining which subset of residues in this region that are unique to the MHV S protein interact specifically with MHV M protein and possibly E protein.

Nature of the host range barrier for coronaviruses. The construction of fMHV is the first example of the complete, reciprocal switch of the host cell specificity of a coronavirus. As such, it contributes a well-defined element to the accumulating proof that the interaction between S protein and receptor is the principal, and perhaps only, determinant of species specificity for coronaviruses. Other elements of this proof come from studies in which it was shown that MHV could evolve, through high-passage persistent infection in tissue culture, to have an expanded host range (1, 52). In these cases, the resulting MHV mutants retained the ability to grow in murine cells but could now also infect cells of a number of other species, presumably via homologs of the murine MHV receptor. Additionally, from the standpoint of the receptor rather than the virus, there have been many demonstrations (including the experiment in Fig. 8B) that expression of the receptor for a given coronavirus in cells of a heterologous, nonpermissive species will render those cells permissive to infection (9, 10, 18, 28, 45, 58, 61).

As mentioned above, fMHV did not appear to be entirely as fit as FIPV with respect to growth in tissue culture (see Results). Although the chimeric S protein allowed the entry of this virus into cells of a heterologous species, it is conceivable that there were also less stringent levels of host species restriction caused by interactions between internal viral components and cytoplasmic host proteins. However, an alternative possibility is that the level of expression of the chimeric S protein was not optimal. Metabolic labeling of RNA synthesis in FCWF cells infected with fMHV revealed that in addition to the expected transcript (RNA3) containing the chimeric S gene, there were at least two transcripts initiating within the chimeric S gene and that these were of similar abundance to

the full-length transcript (data not shown). A complete analysis of these aberrant subgenomic RNAs will be presented elsewhere, but their existence, plus the reduced amount of RNA3 relative to that of the same species in MHV-infected murine cells, is consistent with the notion that transcription of fMHV S mRNA is rate limiting. We previously noted the local derangement of MHV transcription caused by insertion of a heterologous gene into MHV (13), and the observation of a similar effect in fMHV suggests that even the introduction of related coronavirus genetic material into the MHV genome is not entirely tolerated by the transcription apparatus of the virus.

As a direct consequence of the reduced synthesis of RNA3 in fMHV-infected cells, one would expect the relative amount of S protein to be reduced as well. Unfortunately, due to the different efficiencies with which the viral proteins were recognized in immunoprecipitation reactions, we could not draw quantitative conclusions about the relative amounts of S protein synthesis in cells infected by fMHV as compared to MHV and FIPV. However, the relative amounts of radioactivity in the structural proteins of the affinity-purified viruses (Fig. 7) indicate that the chimeric S protein is indeed underrepresented in fMHV. It remains to be established whether this is simply because of the reduced availability of the protein in infected cells or whether it reflects an impaired interaction of the S protein with M, which would also result in less efficient incorporation into viral particles. Obviously, infectivity of particles requires spikes, but nothing is known about the relationship between infectivity and spike content.

Another possible source of the apparent reduced fitness of fMHV may lie in the functionality, rather than the amount, of the chimeric S protein. Earlier expression studies with MHV S gene constructs have indicated that changes in the transmembrane and endodomain can affect the cell-to-cell fusion that this protein causes in susceptible cells (3). Although the chimeric FIPV-MHV S protein clearly exhibits this fusion activity when expressed in feline cells, the efficiency of this process may well be decreased relative to that of the parental wild-type S proteins. If so, this would probably give rise to an inherently lower specific infectivity for fMHV.

Implications for reverse genetics of coronaviruses. For coronaviruses, the extremely large size of the RNA genome has been the main obstacle to generating site-specific mutations for studies of gene expression and function. To date, it has not been possible to construct a full-length cDNA clone of any coronavirus for the production of infectious RNA. Targeted RNA recombination has proved to be a successful alternative approach to the reverse genetics of MHV, and it has been used to generate mutations in the S (13, 32, 42), M (7), E (14), and N (12, 40, 41, 59) genes, gene 4 (13), and the 3′ untranslated region (23, 24) of this virus. This method relies on the ability to select against a temperature-sensitive and thermolabile parent virus in order to identify recombinants that have acquired the mutation of interest through recombination with a transfected donor RNA. In one case (14), mutants were identified by screening rather than selection, but generally, if a recombinant is to be obtained by selection, it cannot be less fit than the recipient virus that is being selected against.

Although fMHV was constructed to begin to answer questions about viral assembly, we believe that this recombinant will also offer a tremendous selective advantage as a recipient virus in targeted recombination. Using a donor RNA containing the original MHV S gene, we expect now to be able to isolate recombinants, no matter how defective, that have regained the ability to grow in murine cells. This new basis for selection should increase even further the strength of this genetic system for MHV. Moreover, this approach should provide a general blueprint for the generation of genomic mutations in the structural genes of any coronavirus.

ACKNOWLEDGMENTS

We are grateful to Cheri Koetzner for expert technical assistance and to Matthew Shudt and Tim Moran of the Molecular Genetics Core Facility of the Wadsworth Center for the synthesis of oligonucleotides and automated DNA sequencing. We also thank John Fleming, Wayne Corapi, and Tsutomu Hohdatsu for providing antibodies. We are grateful to John Rossen, Harry Vennema, and Xander de Haan for their constructive support.

This work was supported in part by Public Health Service grant AI 39544 from the National Institutes of Health to P.S.M.

REFERENCES

1. **Baric, R. S., B. Yount, L. Hensley, S. A. Peel, and W. Chen.** 1997. Episodic evolution mediates interspecies transfer of a murine coronavirus. J. Virol. **71:**1946–1955.
2. **Baudoux, P., C. Carrat, L. Besnardeau, B. Charley, and H. Laude.** 1998. Coronavirus pseudoparticles formed with recombinant M and E proteins induce alpha interferon synthesis by leukocytes. J. Virol. **72:**8636–8643.
3. **Bos, E. C. W., L. Heijnen, W. Luytjes, and W. J. M. Spaan.** 1995. Mutational analysis of the murine coronavirus spike protein: effect on cell-to-cell fusion. Virology **214:**453–463.
4. **Bos, E. C. W., W. Luytjes, H. van der Meulen, H. K. Koerten, and W. J. M. Spaan.** 1996. The production of recombinant infectious DI-particles of a murine coronavirus in the absence of helper virus. Virology **218:**52–60.
5. **Bos, E. C. W., W. Luytjes, and W. J. M. Spaan.** 1997. The function of the spike protein of mouse hepatitis virus strain A59 can be studied on virus-like particles: cleavage is not required for infectivity. J. Virol. **71:**9427–9433.
6. **de Groot, R. J., J. Maduro, J. A. Lenstra, M. C. Horzinek, B. A. M. van der Zeijst, and W. J. M. Spaan.** 1987. cDNA cloning and sequence analysis of the gene encoding the peplomer protein of feline infectious peritonitis virus. J. Gen. Virol. **68:**2639–2646.
7. **de Haan, C. A. M., L. Kuo, P. S. Masters, H. Vennema, and P. J. M. Rottier.** 1998. Coronavirus particle assembly: primary structure requirements of the membrane protein. J. Virol. **72:**6838–6850.
8. **de Haan, C. A. M., P. Roestenberg, M. de Wit, A. A. F. de Vries, T. Nilsson, H. Vennema, and P. J. M. Rottier.** 1998. Structural requirements for O-glycosylation of the mouse hepatitis virus membrane protein. J. Biol. Chem. **273:**29905–29914.
9. **Delmas, B., J. Gelfi, R. L'Haridon, L. K. Vogel, H. Sjöström, O. Norén, and H. Laude.** 1992. Aminopeptidase N is a major receptor for the enteropathogenic coronavirus TGEV. Nature **357:**417–420.
10. **Dveksler, G. S., M. N. Pensiero, C. B. Cardellichio, R. W. Williams, G.-S. Jiang, K. V. Holmes, and C. W. Dieffenbach.** 1991. Cloning of the mouse hepatitis virus (MHV) receptor: expression in human and hamster cell lines confers susceptibility to MHV. J. Virol. **65:**6881–6891.
11. **Fichot, O., and M. Girard.** 1990. An improved method for sequencing of RNA templates. Nucleic Acids Res. **18:**6162.
12. **Fischer, F., D. Peng, S. T. Hingley, S. R. Weiss, and P. S. Masters.** 1997. The internal open reading frame within the nucleocapsid gene of mouse hepatitis virus encodes a structural protein that is not essential for viral replication. J. Virol. **71:**996–1003.
13. **Fischer, F., C. F. Stegen, C. A. Koetzner, and P. S. Masters.** 1997. Analysis of a recombinant mouse hepatitis virus expressing a foreign gene reveals a novel aspect of coronavirus transcription. J. Virol. **71:**5148–5160.
14. **Fischer, F., C. F. Stegen, P. S. Masters, and W. A. Samsonoff.** 1998. Analysis of constructed E gene mutants of mouse hepatitis virus confirms a pivotal role for E protein in coronavirus assembly. J. Virol. **72:**7885–7894.
15. **Fleming, J. O., R. A. Shubin, M. A. Sussman, N. Casteel, and S. A. Stohlman.** 1989. Monoclonal antibodies to the matrix (E1) glycoprotein of mouse hepatitis virus protect mice from encephalitis. Virology **168:**162–167.

15a. **Godeke, G.-J., C. A. M. de Haan, J. W. A. Rossen, H. Vennema, and P. J. M. Rottier.** 1999. Assembly of spikes into coronavirus particles is mediated by the carboxy-terminal domain of the spike protein. J. Virol. **74:**1566–1571.

16. **Godet, M., J. Grosclaude, B. Delmas, and H. Laude.** 1994. Major receptor-binding and neutralization determinants are located within the same domain of the transmissible gastroenteritis virus (coronavirus) spike protein. J. Virol. **68:**8008–8016.
17. **Godet, M., R. L'haridon, J.-F. Vautherot, and H. Laude.** 1992. TGEV corona virus ORF4 encodes a membrane protein that is incorporated into virions. Virology **188:**666–675.
18. **Hansen, G. H., B. Delmas, L. Besnardeau, L. K. Vogel, H. Laude, H. Sjöström, and O. Norén.** 1998. The coronavirus transmissible gastroenteritis

virus causes infection after receptor-mediated endocytosis and acid-dependent fusion with an intracellular compartment. J. Virol. **72:**527–534.
19. **Hegyi, A., and A. F. Kolb.** 1998. Characterization of determinants involved in the feline infectious peritonitis virus receptor function of feline aminopeptidase N. J. Gen. Virol. **79:**1387–1391.
20. **Hohdatsu, T., Y. Izumiya, Y. Yokoyama, K. Kida, H. Koyama.** 1998. Differences in virus receptor for type I and type II feline infectious peritonitis virus. Arch. Virol. **143:**839–850.
21. **Holmes, K. V., E. W. Dollar, and L. S. Sturman.** 1981. Tunicamycin resistant glycosylation of a coronavirus glycoprotein: demonstration of a novel type of viral glycoprotein. Virology **115:**334–344.
22. **Horton, R. M., and L. R. Pease.** 1991. Recombination and mutagenesis of DNA sequences using PCR, p. 217–247. *In* M. J. McPherson (ed.), Directed mutagenesis: a practical approach. IRL Press, New York, N.Y.
23. **Hsue, B., and P. S. Masters.** 1997. A bulged stem-loop structure in the 3′ untranslated region of the genome of the coronavirus mouse hepatitis virus is essential for replication. J. Virol. **71:**7567–7578.
24. **Hsue, B., and P. S. Masters.** 1999. Insertion of a new transcriptional unit into the genome of mouse hepatitis virus. J. Virol. **73:**6128–6135.
25. **Kingsman, S. M., and C. E. Samuel.** 1980. Mechanism of interferon action. Interferon-mediated inhibition of simian virus-40 early RNA accumulation. Virology **101:**458–465.
26. **Klumperman, J., J. Krijnse Locker, A. Meijer, M. C. Horzinek, H. J. Geuze, and P. J. M. Rottier.** 1994. Coronavirus M proteins accumulate in the Golgi complex beyond the site of virion budding. J. Virol. **68:**6523–6534.
27. **Koetzner, C. A., M. M. Parker, C. S. Ricard, L. S. Sturman, and P. S. Masters.** 1992. Repair and mutagenesis of the genome of a deletion mutant of the coronavirus mouse hepatitis virus by targeted RNA recombination. J. Virol. **66:**1841–1848.
28. **Kolb, A. F., A. Hegyi, and S. G. Siddell.** 1997. Identification of residues critical for the human coronavirus 229E receptor function of human aminopeptidase N. J. Gen. Virol. **78:**2795–2802.
29. **Kubo, H., Y. K. Yamada, and F. Taguchi.** 1994. Localization of neutralizing epitopes and the receptor-binding site within the amino-terminal 330 amino acids of the murine coronavirus spike protein. J. Virol. **68:**5403–5410.
30. **Laemmli, U. K.** 1970. Cleavage of structural proteins during the assembly of the head of bacteriophage T4. Nature (London) **227:**680–685.
31. **Laude, H., and P. S. Masters.** 1995. The coronavirus nucleocapsid protein, p. 141–163. *In* S. G. Siddell (ed.), The Coronaviridae. Plenum Press, New York, N.Y.
32. **Leparc-Goffart, I., S. T. Hingley, M. M. Chua, J. Phillips, E. Lavi, and S. R. Weiss.** 1998. Targeted recombination within the spike gene of murine coronavirus mouse hepatitis virus-A59: Q159 is a determinant of hepatotropism. J. Virol. **72:**9628–9636.
33. **Liu, D. X., and S. C. Inglis.** 1991. Association of the infectious bronchitis virus 3c protein with the virion envelope. Virology **185:**911–917.
34. **Luytjes, W., P. J. Bredenbeek, A. F. H. Noten, M. C. Horzinek, and W. J. M. Spaan.** 1988. Sequence of mouse hepatitis virus A59 mRNA2: Indications for RNA recombination between coronaviruses and influenza C virus. Virology **166:**415–422.
35. **Masters, P. S., C. A. Koetzner, C. A. Kerr, and Y. Heo.** 1994. Optimization of targeted RNA recombination and mapping of a novel nucleocapsid gene mutation in the coronavirus mouse hepatitis virus. J. Virol. **68:**328–337.
36. **Nguyen, V.-P., and B. Hogue.** 1997. Protein interactions during coronavirus assembly. J. Virol. **71:**9278–9284.
37. **Olsen, C. W., W. V. Corapi, C. K. Ngichabe, J. D. Baines, and F. W. Scott.** 1992. Monoclonal antibodies to the spike protein of feline infectious peritonitis virus mediate antibody-dependent enhancement of infection of feline macrophages. J. Virol. **66:**956–965.
38. **Opstelten, D.-J. E., P. de Groote, M. C. Horzinek, H. Vennema, and P. J. M. Rottier.** 1993. Disulfide bonds in folding and transport of mouse hepatitis coronavirus glycoproteins. J. Virol. **67:**7394–7401.
39. **Opstelten, D.-J. E., M. J. B. Raamsman, K. Wolfs, M. C. Horzinek, and P. J. M. Rottier.** 1995. Envelope glycoprotein interactions in coronavirus assembly. J. Cell Biol. **131:**339–349.
40. **Peng, D., C. A. Koetzner, and P. S. Masters.** 1995. Analysis of second-site revertants of a murine coronavirus nucleocapsid protein deletion mutant and construction of nucleocapsid protein mutants by targeted RNA recombination. J. Virol. **69:**3449–3457.
41. **Peng, D., C. A. Koetzner, T. McMahon, Y. Zhu, and P. S. Masters.** 1995. Construction of murine coronavirus mutants containing interspecies chimeric nucleocapsid proteins. J. Virol. **69:**5475–5484.
42. **Phillips, J. J., M. M. Chua, E. Lavi, and S. R. Weiss.** 1999. Pathogenesis of chimeric MHV4/MHV-A59 recombinant viruses: the murine coronavirus spike protein is a major determinant of neurovirulence. J. Virol. **73:**7752–7760.
43. **Risco, C., I. M. Antón, L. Enjuanes, and J. L. Carrascosa.** 1996. The transmissible gastroenteritis coronavirus contains a spherical core shell consisting of M and N proteins. J. Virol. **70:**4773–4777.
44. **Risco, C., M. Muntión, L. Enjuanes, and J. L. Carrascosa.** 1998. Two types of virus-related particles are found during transmissible gastroenteritis virus morphogenesis. J. Virol. **72:**4022–4031.
45. **Rossen, J. W. A., C. P. J. Bekker, G. J. A. M. Strous, M. C. Horzinek, G. S. Dveksler, K. V. Holmes, and P. J. M. Rottier.** 1996. A murine and a porcine coronavirus are released from opposite surfaces of the same epithelial cells. Virology **224:**345–351.
46. **Rossen, J. W. A., W. F. Voorhout, M. C. Horzinek, A. van der Ende, G. J. A. M. Strous, and P. J. M. Rottier.** 1995. MHV-A59 enters polarized murine epithelial cells through the apical surface but is released basolaterally. Virology **210:**54–66.
47. **Rottier, P., J. Armstrong, and D. I. Meyer.** 1985. Signal recognition particle-dependent insertion of coronavirus E1, an intracellular membrane glycoprotein. J. Biol. Chem. **260:**4648–4652.
48. **Rottier, P. J. M.** 1995. The coronavirus membrane glycoprotein, p. 115–139. *In* S. G. Siddell (ed.), The Coronaviridae. Plenum Press, New York, N.Y.
49. **Rottier, P. J. M., M. C. Horzinek, and B. A. M. van der Zeijst.** 1981. Viral protein synthesis in mouse hepatitis virus strain A59-infected cells: effects of tunicamycin. J. Virol. **40:**350–357.
50. **Sambrook, J., E. F. Fritsch, and T. Maniatis.** 1989. Molecular cloning: a laboratory manual, 2nd ed. Cold Spring Harbor Laboratory Press, Cold Spring Harbor, N.Y.
51. **Sanger, F., S. Nicklen, and A. R. Coulson.** 1977. DNA sequencing with chain terminating inhibitors. Proc. Natl. Acad. Sci. USA **74:**5463–5467.
52. **Schickli, J. H., B. D. Zelus, D. E. Wentworth, S. G. Sawicki, and K. V. Holmes.** 1997. The murine coronavirus mouse hepatitis virus strain A59 from persistently infected murine cells exhibits an extended host range. J. Virol. **71:**9499–9507.
53. **Senanayake, S. D., M. A. Hofmann, J. L. Maki, and D. A. Brian.** 1992. The nucleocapsid protein gene of bovine coronavirus is bicistronic. J. Virol. **66:**5277–5283.
54. **Shieh, C.-K., H.-J. Lee, K. Yokomori, N. La Monica, S. Makino, and M. M. C. Lai.** 1989. Identification of a new transcription initiation site and the corresponding functional gene 2b in the murine coronavirus RNA genome. J. Virol. **63:**3729–3736.
55. **Siddell, S. G.** 1995. The Coronaviridae: an introduction, p. 1–10. *In* S. G. Siddell (ed.), The Coronaviridae. Plenum Press, New York, N.Y.
56. **Sturman, L. S.** 1977. Characterization of a coronavirus. I. Structural proteins: effects of preparative conditions on the migration of protein in polyacrylamide gels. Virology **77:**637–649.
57. **Tooze, J., S. A. Tooze, and G. Warren.** 1984. Replication of coronavirus MHV-A59 in Sac$^-$ cells: determination of the first site of budding of progeny virions. Eur. J. Cell Biol. **33:**281–293.
58. **Tresnan, D. B., R. Levis, and K. V. Holmes.** 1996. Feline aminopeptidase N serves as a receptor for feline, canine, porcine and human coronaviruses in serogroup I. J. Virol. **70:**8669–8674.
59. **van der Most, R. G., L. Heijnen, W. J. M. Spaan, and R. J. de Groot.** 1992. Homologous RNA recombination allows efficient introduction of site-specific mutations into the genome of coronavirus MHV-A59 via synthetic co-replicating RNAs. Nucleic Acids Res. **20:**3375–3381.
60. **Vennema, H., G.-J. Godeke, J. W. A. Rossen, W. F. Voorhout, M. C. Horzinek, D.-J. E. Opstelten, and P. J. M. Rottier.** 1996. Nucleocapsid-independent assembly of coronavirus-like particles by co-expression of viral envelope protein genes. EMBO J. **15:**2020–2028.
61. **Yeager, C. L., R. A. Ashmun, R. K. Williams, C. B. Cardellichio, L. H. Shapiro, A. T. Look, and K. V. Holmes.** 1992. Human aminopeptidase N is a receptor for human coronavirus 229E. Nature **357:**420–422.
62. **Yu, X., W. Bi, S. R. Weiss, and J. L. Leibowitz.** 1994. Mouse hepatitis virus gene 5b protein is a new virion envelope protein. Virology **202:**1018–1023.